Title	Frequency dynamics during high CCGT and wind penetrations
Authors(s)	Meegahapola, Lasantha, Flynn, Damian
Publication date	2011
Publication information	Meegahapola, Lasantha, and Damian Flynn. "Frequency Dynamics during High CCGT and Wind Penetrations." IEEE, 2011.
Conference details	Presented at AUPEC 2011, Australasian Universities Power Engineering Conference, Brisbane, Australia, 25 - 28 September 2011
Publisher	IEEE
Item record/more information	http://hdl.handle.net/10197/3553
Publisher's statement	© 2011 IEEE. Personal use of this material is permitted. Permission from IEEE must be obtained for all other uses, in any current or future media, including reprinting/republishing this material for advertising or promotional purposes, creating new collective works, for resale or redistribution to servers or lists, or reuse of any copyrighted component of this work in other works.

Frequency Dynamics during High CCGT and Wind Penetrations

Lasantha Meegahapola, *Member, IEEE*, and Damian Flynn, *Member, IEEE*

Abstract— Frequency stability is the paramount concern for secure and reliable operation of a power system. High wind penetration levels are reported in power systems with high thermal generation, and hence its likely to result high wind and combined-cycle gas turbine (CCGT) penetrations during system operation since CCGTs are the most preferable choice for the thermal generation. The doubly-fed induction generators (DFIGs) do not provide any inertial response while the CCGTs have unique frequency response during the system frequency disturbances. Therefore, CCGT turbine response characteristics and the zero inertial response may influence on frequency dynamics of a power network. The main objective of this study is to analyze the frequency dynamics during generator outages and three-phase short-circuit faults in a power network with high CCGT and wind penetrations. A test network model was developed based on the Northern-Ireland network in DIgSILENT Power Factory software package. It has shown that frequency stability may be threatened when three-phase short circuit faults occur in power networks during high CCGT and wind penetrations which may lead to CCGT combustor lean-blowout and ultimately results large frequency excursions in the network.

Index Terms— CCGT, DFIG, frequency nadir, frequency stability, lean blowout, ROCOF.

I. INTRODUCTION

During recent years wind integration into power networks has increased significantly as the pioneering renewable energy source for electricity generation. In year 2010, 38.3 GW wind generation capacity was installed in power networks around the world while indicating a 24.1% increase in wind power capacity [1]. Large scale wind farm developments became mainly popular in thermal power network to achieve the binding targets imposed by the various policy directives on reducing green-house gas emissions from electricity generation [2].

At present, the combined-cycle gas turbine (CCGT) is the most preferable thermal generation option due to its high generation efficiency, flexibility and lower emissions compared to other thermal generation sources. The CCGT dynamic behaviour during system disturbances is different from the other thermal generating units, and hence may cause considerable impact during frequency excursions [3]. Large

frequency excursions during grid faults have given rise to alarming security issues in power systems. As an example, a recent incident in 2008, which occurred in the Florida power system, resulting in a large number of generators (4300 MW) and customer loads (3650 MW) being disconnected from the grid [4]. Six of the CCGT generator units were disconnected due to a phenomena called turbine combustor 'lean-blowout', which occurs as a consequence of compressor speed increase (this will increase the airflow to the combustion chamber) and governor control action (fuel reduction) during a frequency excursion in the system [5].

In terms of wind generation, power electronics based variable-speed wind generators (e.g. doubly-fed induction generator (DFIG), direct-drive synchronous generator (DDSG)) are the preferable choice for wind farm developments at present, and its more likely to achieve high wind penetrations based on DFIGs. However, these generating units are inherently less responsive to system frequency dynamics since their mechanical dynamics are decoupled from electromagnetic dynamics by the power electronics converter system [6]. And ultimately, these units could not able to deliver inertial response during frequency excursions while leading to frequency stability problems in the network.

With the large scale integration of wind power into thermal based power systems its likely to result high DFIG and CCGT penetrations during system operation. Therefore, with high wind and CCGT penetrations it is essential to analyze the wind power and CCGT interactions during frequency events in the network. This paper primarily focuses on analyzing the frequency stability impact of a test system based on Northern Ireland (NI) power network during high CCGT and wind penetrations in a power network.

II. CHARACTERIZATION OF FREQUENCY DYNAMICS

This section characterizes various types of frequency dynamics in a power network. System frequency dynamics during system disturbances can be classified into three different types: frequency dynamics following a generator outage event; a transient grid fault without fault resistance; and a transient grid fault with fault resistance (see Fig. 1). Fig. 1 illustrates the frequency variations during a generator outage event and a 150 ms three-phase short-circuit fault in a network.

During a generator outage event, system frequency reduces due to a decrease in power generation in the network before recovering to a steady-state value. In terms of a transient grid fault (without fault resistance), initially system frequency increases due to a reduction in load demand (due to voltage reduction in a wide-area of the network). Consequently, system frequency reduces due to generator tripping (in

particular, wind generation) and the turbine governor control action of the generators.
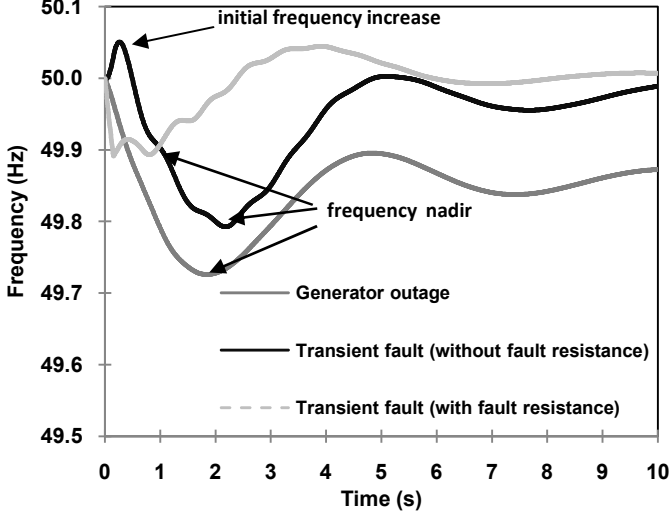

Fig. 1: Frequency dynamics during different system events.

The frequency response during a grid fault further depends on the voltage dependency of the power system loads. When a fault occurs with a fault resistance a frequency drop will result following the fault. This can be represented as follows:

$$P_G < P_L + P_{Loss} + P_F$$

where, P_G, P_L, P_{Loss} and P_F represent total active power generation, active power consumed by system loads, active power losses and active power consumed by the fault. The active power consumed by the fault can be represented as follows:

$$P_F = I_F^2.R_F$$

where, I_f and R_f represent the fault current and fault resistance respectively. When a fault occurs without effective fault resistance the frequency will increase, although fault current is flowing in the system, and this can be represented as follows:

$$P_G > P_L + P_{Loss}$$

However, the power consumption of the system loads (P_L) depends on the load behaviour, and therefore a frequency increase or decrease will further depend on the load characteristics of the system [7-8].

III. TEST NETWORK MODELLING ASPECTS AND SCENARIO FORMULATION

This section provides a basic overview of the test system modelling aspects, the study assumptions, and the scenario formulation for frequency stability analysis.

A. Test Network

Aforementioned the test network designed for this study is based on NI network [9] which is comprised of 2202 MW of installed conventional generation capacity and 282.85 MW of installed wind generation capacity. A schematic diagram of the test network is shown in Fig. 2.
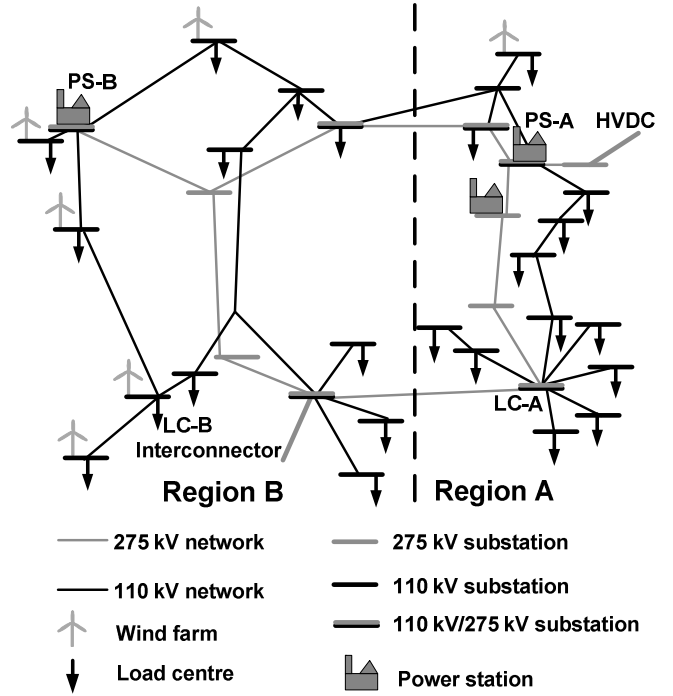

Fig. 2: Test network model.

Test network is consisted of two interconnectors (500 MW high-voltage direct-current (HVDC)) and 600 MW link). The dynamic network simulation model was developed within the DIgSILENT Power Factory software package. The test system is comprised of two voltage levels, namely 110 kV and 275 kV, and developed with 110 kV and 275 kV substations with 110/33 kV step-down transformers. The loads and wind power plants are represented at 33 kV to analyze voltage variations in the distribution network during transient grid faults. The wind generators are grid connected via 0.69/33 kV step-up transformer. The HVDC interconnector was modeled using a conventional synchronous generator with zero inertia constant, while the other interconnector was modeled using a conventional synchronous generator equipped with a standard IEEE governor and static exciter model. The inertia constant for the equivalent generator was set at 6 s and the governor droop was set at 4%. The wind technology mix for base case is FSIG:DFIG/ 40:60 (i.e. FSIG: 114.85 MW/ DFIG: 168 MW). The test network was formed as two network regions (see Fig. 2) which is based on the following criteria:

1. High demand, low wind region (Region-A)
2. Low demand, high wind region (Region-B)

The synchronous generation portfolio of the test network is comprised of CCGT units, open-cycle gas turbine (OCGT) units, and steam turbine (ST) units using both coal and heavy fuel oil (HFO). During system operation, the ratio between synchronous generation and wind generation may change based on the available wind output. During high wind penetrations it is more likely to result in a wind rich region in Region-B which may create stability concerns at such times. The conventional units are dispatched based on economic dispatch.

B. Scenario Formulation

The following fault locations were chosen to analyze large disturbance stability issues in the test network (see Fig. 2).

1. Power Station – A (PS-A) (CCGT, OCGT, ST)
2. Power Station – B (PS-B) (CCGT, OCGT)
3. Load Centre – A (LC-A)
4. Load Centre – A (LC-A)

The fault locations were selected by considering the defined network regions, transmission voltage levels, and proximity to synchronous generators, wind generators and load centres in the network. In addition, 10% and 100% wind farm loading has also been analyzed in the study. The synchronous generation, wind generation and system load for each wind farm loading levels are illustrated in Fig. 3.
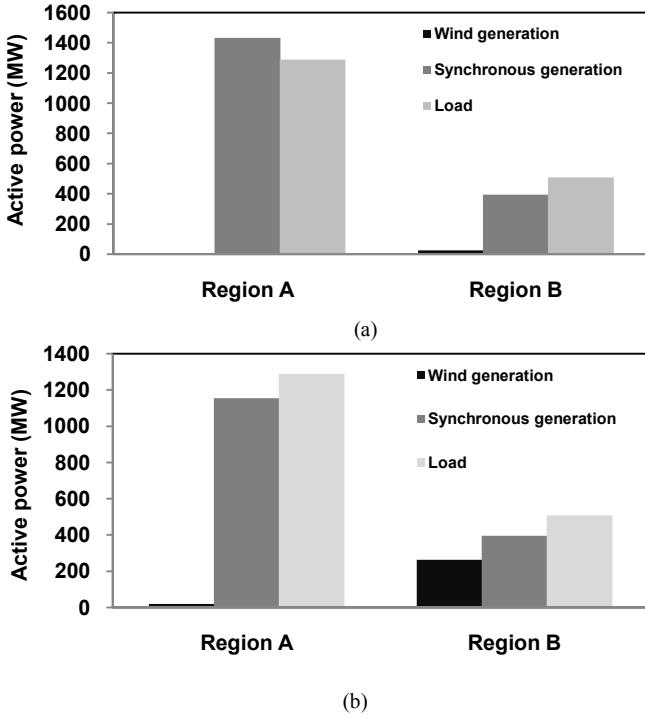

(a)

(b)

Fig. 3: Generation portfolio for each region: (a) 10% wind; (b) 100% wind

During 100% wind farm loading excess generation in Region-B is exported to Region-A. However, at 10% wind farm loading, Region-A exports power to Region-B to balance the power deficit in the region. Therefore, system has high inter-area power flows between the regions A and B. The 100% wind farm loading in the test network is unlikely; however objective is to illustrate the implications of the worst case scenario during high wind penetration. The 100% static load model has been used in the dynamic simulation model.

IV. FREQUENCY DYNAMICS DURING GRID DISTURBANCES

System frequency stability was analyzed by considering three-phases short-circuit and generator outage events in the network.

A. Frequency Dynamic during Three-Phase Short-Circuit

The first scenario, frequency stability was analyzed following a 150 ms three-phase short-circuit fault at the four network nodes defined in the previous section. The rate-of-

change-of-frequency (ROCOF) was calculated during the initial frequency increase and frequency decrease following a fault in the network. The 100% static load model was used in this study, while two wind farm loading levels were considered (i.e. 10% and 100% wind farm loading). The calculated maximum ROCOF for the initial frequency increase and during frequency decrease are illustrated in Table I.

Table I: ROCOF during Three-Phase Short-Circuit Faults with Different Wind Farm Loading Levels

Event	ROCOF (Hz/s) (during increase)		ROCOF (Hz/s) (during decrease)	
	Region		Region	
	A	B	A	B
275 kV PS-A 10% loading	1.00	1.06	-0.76	-0.74
275 kV PS-A: 100% loading	1.20	1.28	-0.83	-0.80
275 kV PS-B: 10% loading	0.41	0.41	-0.22	-0.22
275 kV PS-B: 100% loading	0.40	0.48	—	—
110 kV LC-A: 10% loading	0.30	0.31	-0.12	-0.12
110 kV LC-A: 100% loading	0.32	0.31	-0.13	-0.13
110 kV LC-B: 10% loading	0.11	0.11	—	—
110 kV LC-B: 100% loading	0.05	0.03	-0.24	-0.24

A negative ROCOF results when generation is insufficient to balance the load demand in the system, while a positive ROCOF results when an active power surplus exists in the system. According to Table I, significantly high initial ROCOFs are seen when faults occur at the 275 kV network nodes, since they cause a detrimental impact on bus voltages, and ultimately result in a large instantaneous reduction in system demand following the fault. This causes an instantaneous increase in system frequency due to the large generation-demand imbalance in the system. As an example, at 100% wind farm loading, when a fault occurs at the PS-A 275 kV busbar a ROCOF of 1.2 Hz/s (Region A) is incurred, while the corresponding ROCOF when a fault occurs at the LC-A 110 kV busbar (Region-B) is 0.32 Hz/s. However, the impact of governor response for the initial frequency excursion is insignificant, since the frequency increase occurs for less than 0.5 s following fault inception in the network.
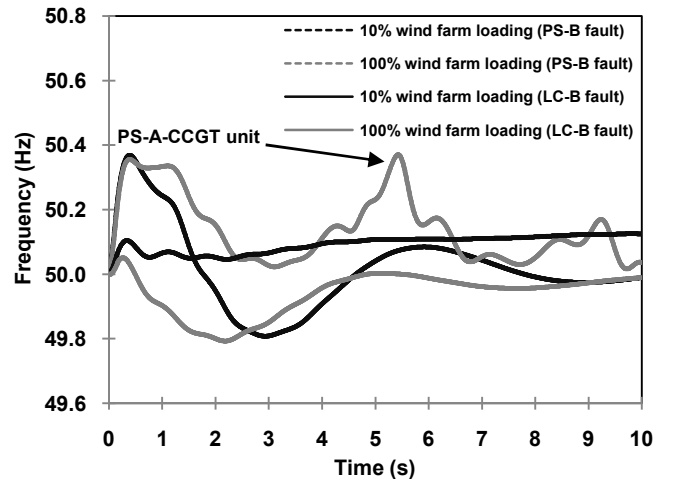

Fig. 4: Frequency variation at the PS-A following grid faults

System frequency continuously increases when a fault occurs at the LC-B 110 kV busbar (10% wind farm loading) and system frequency remains above 50 Hz when a fault

occurs at the PS-B 275 kV busbar (100% wind farm loading) (see Fig. 4). Frequency variations in Region-A (at the PS-A) for both these incidents are illustrated in Fig. 4. As illustrated in Fig. 4, both at a PS-B 275 kV fault (100% wind farm loading) and LC-B 110 kV fault (10% wind farm loading) the system frequency continuously increases. During the above two incidents the active power generation of the generator units reduces following the fault (although the total generation exceeds the total demand in the system) due to significant voltage collapse at the generator terminal (in particular, at one of the PS-B CCGT units). This leads to an increase in the accelerating torque (difference between the mechanical torque and the electrical torque of the generator) of the generators following fault clearance, due to comparatively high mechanical torque input to the generator. The mechanical torque increase is mainly due to the unique turbine response of the CCGTs, which will be discussed later.

The accelerating torque causes the synchronous generator speed to increase, and hence the system frequency continuously increases. In these two incidents (LC-B and PS-B faults) the average accelerating power is non-zero following the fault, and hence the CCGT continues to accelerate while increasing the frequency in the network. During the other instances following fault clearance, the generator terminal voltage gradually increases, and ultimately the generator active power output recovers while reducing the accelerating toque to zero. Consequently, the generator speed stabilises while allowing the turbine to stabilise its active power output during post-fault period. A comparison of the PS-A CCGT acceleration torque for different scenarios is illustrated in Fig. 5.
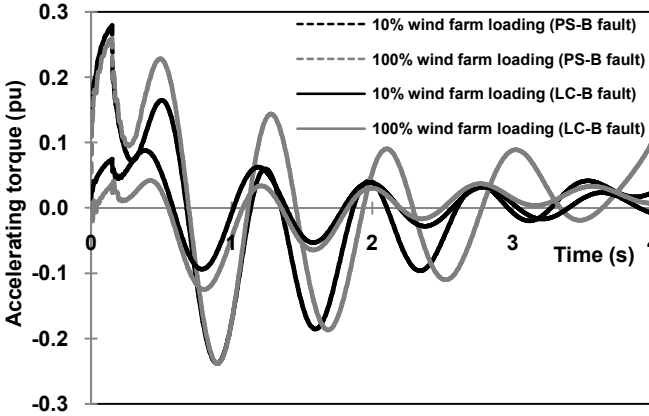

Fig. 5: PS-A-CCGT unit accelerating torque during a fault

As illustrated in Fig. 5, the average accelerating torque is positive (5 s following fault inception) for a fault at the PS-B 275 kV busbar at 100% wind farm loading and for a fault at the LC-B 110 kV busbar at 10% wind farm loading. In addition, when a fault occurs at the PS-B 275 kV busbar during 100% wind farm loading, due to the voltage reduction across a large area (an area with high wind resources-Region B) there is a high reactive power absorption (mainly FSIGs) from the grid, and hence the voltage recovery process during the post-fault period is much slower compared to the 10% wind farm loading (see Fig. 6). This results in the generator electrical torque reducing while increasing the accelerating torque of the generator. A comparison of the PS-A CCGT terminal voltage for the above scenarios is illustrated in Fig. 6.
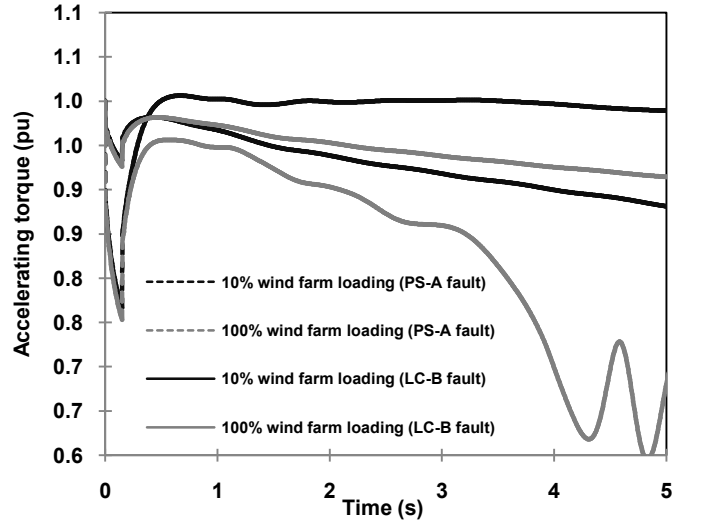

Fig. 6: PS-A 275 kV bus voltage variation during a fault at the PS-B 275 kV bus

In addition, CCGT turbine dynamics also contribute to a large frequency increase in the system following fault clearance. A frequency increase during a grid fault (due to the instantaneous generation-demand imbalance) causes an increase of the CCGT compressor speed, since it is directly synchronised with the grid. As a result airflow to the combustion chamber is increased, and hence the pressure across gas turbine is increased while increasing the turbine power output [3]. Therefore, the power output of the CCGT units increases following a grid fault while increasing the accelerating torque of the generator. Furthermore, generator governor action limits the fuel flow to the combustor and together with the compressor speed increase may lead to a turbine combustor 'lean-blowout' situation or a flameout condition as happened in the Florida power network [4]. During other instances, such as a fault at the PS-A 275 kV busbar at 100% wind farm loading, the same phenomena (PS-B 275 kV busbar fault at 100% wind farm loading) continues for 1 to 1.5 s, nevertheless the subsequent recovery of the bus voltages enables a quick reduction in accelerating torque, and hence the generator speed stabilises at a steady-state value.

A large negative ROCOF can be seen during a frequency decrease when a fault occurs on the 275 kV network (PS-A 275 kV busbar and PS-B busbar) and in close proximity to high wind resources (100% wind farm loading at LC-B 110 kV busbar). A large negative ROCOF has mainly occurred due to two reasons:

i. Wind farm disconnection (due to activation of over-speed protection and low-voltage protection) and slow recovery response of the wind generators following fault clearance [10]. The reactive power demand of the accelerated wind generators will also affect the bus voltages, and hence the power output of the generator. In addition, online DFIG units do not provide inertial response during frequency decrease, and hence will also affect frequency stability of the system.

ii. The unique CCGT response during frequency excursions also exacerbates the frequency dynamics in the system [3].

The frequency impact due to CCGT response can be exemplified as follows: during frequency decrease, the compressor slows down since it is directly synchronized with the grid. The reduction in compressor speed results in a reduction in the pressure ratio of the compressor, and hence the airflow into the combustion chamber is reduced. The reduction in fuel-to-air ratio results in a reduction in gas turbine pressure and ultimately turbine power output is reduced. If these units are operating below maximum power output (i.e. below base-load operation), variable inlet guide vanes (IGVs) adjust the fuel to air ratio by increasing the airflow to the compressor. These units are designed to maintain the optimum exhaust gas temperature to maintain maximum efficiency of the combined unit (in particular, the efficiency of the ST section) [3]. The impact due to CCGT response can be understood from Fig. 7, which illustrates the turbine response of two PS-A generators (steam turbine (ST) and a CCGT) and the PS-A frequency following a three-phase short-circuit fault at the PS-A 275 kV busbar.
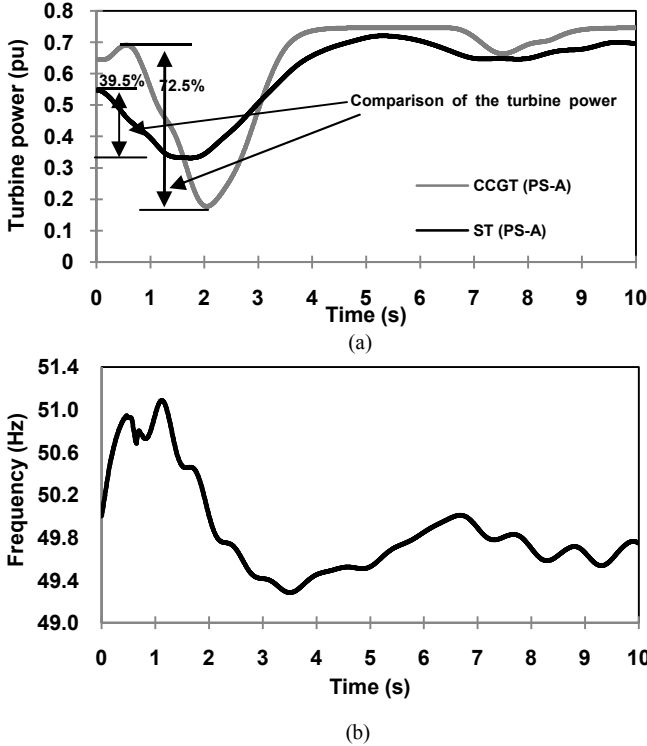

(a)

(b)

Fig. 7: PS-A dynamic following a fault at the PS-A 275 kV busbar: (a) generators turbine power output; (b) system frequency.

According to Fig. 7, when a fault occurs at the PS-A 275 kV busbar, the CCGT power output reduced by 72.5%, while the ST power output only reduced by 39.5%. Therefore, it is apparent that CCGT unique turbine response also influences a large ROCOF and a frequency nadir (see Table I) due to its steep decrease in turbine power output. The wind and CCGT penetrations (as a percentage of total system demand) at two different wind farm loading levels are illustrated in Table II.

Table II: Wind and CCGT Penetrations for Different Wind Farm Loading Levels

	10% wind farm loading	100% wind farm loading
Total wind	1.57%	15.72%
CCGT	47.56%	47.56%

According to Table II, the system is comprised of high CCGT and wind penetration, particularly at 100% wind farm loading, and hence the aforementioned dynamic impact of wind and CCGTs are much dominant at 100% wind farm loading. Therefore, it results a high ROCOF and a frequency nadir during 100% wind farm loading in comparison to 10% wind farm loading (see Table I-during frequency decrease).

However, if the CCGTs are operating at maximum power output (base-load), IGVs can no longer compensate the fuel to air ratio, and hence the fuel to air ratio increases while increasing the exhaust gas temperature. This increase is detected by the temperature control system and ultimately reduces the fuel flow to the combustor while reducing the overall output of the combined unit [3]. If these units are operating at base-load, the above frequency excursions may be detrimental. To illustrate this impact, an additional, scenario was considered with base-load CCGT units in the system with a generator outage event at the PS-A power station at 100% wind farm loading. Therefore, two PS-A CCGT units were operated at the base load to compare the frequency impact on system. A variation of Region-A frequency for a PS-A generator outage event with, and without, base-load CCGT units is illustrated in Fig. 8.
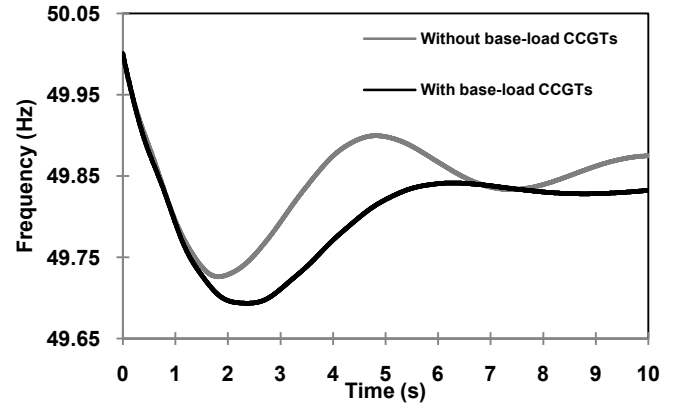

Fig. 8: Comparison of the Region-A frequency with and without base-load CCGTs in the system.

As illustrated in Fig. 8, frequency nadir has decreased from 49.73 Hz to 49.69 Hz when CCGT units are operating at base-load. Therefore a detrimental impact can be expected under such circumstances. Frequency nadir observed following grid faults are given in Table III.

Table III: Frequency Nadir during Grid Faults with Different Wind Farm Loading Levels

Event	Frequency nadir (Hz)	
	Region-A	Region-B
275 kV PS-A: 10% loading	49.35	49.36
275 kV PS-A: 100% loading	49.28	49.31
275 kV PS-B: 10% loading	49.81	49.81
275 kV PS-B: 100% loading	—	—
110 kV LC-A: 10% loading	49.89	49.89
110 kV LC-A: 100% loading	49.88	49.89
110 kV LC-B: 10% loading	—	—
110 kV LC-B: 100% loading	49.79	49.79

As illustrated in Table III, a much more severe frequency nadir is seen when a fault occurs at the PS-A 275 kV busbar, since it causes the most detrimental impact on the PS-A generator units as mentioned in the early parts of the section.

B. Frequency Dynamic during Generator Outages

In the second scenario, frequency stability was analyzed following a generator outage event in each region with different wind farm loading levels. The 100% static load model was used in this study, while two wind farm loading levels were considered (i.e. 10% and 100% wind farm loading). The generator outages were simulated at the PS-A and the PS-B power stations, and the active power deficit is same for both outages. The resulting ROCOF and frequency nadir following generator outages are illustrated in Table IV.

Table IV: ROCOF and Frequency Nadir during Generator Outages

Event	ROCOF (Hz/s)		Frequency nadir (Hz)	
	Region		Region	
	A	B	A	B
PS-A outage: 10% loading	-0.30	-0.30	49.75	49.75
PS-A outage: 100% loading	-0.32	-0.32	49.73	49.73
PS-B outage: 10% loading	-0.28	-0.29	49.76	49.76
PS-B outage: 100% loading	-0.32	-0.32	49.73	49.72

As indicated in Table IV, when a generator outage occurs at the wind rich region (Region-B, PS-B power station) frequency stability impact is small compared to a generator outage in the low wind region (Region-A, PS-A power station). As an example, at 10% wind farm loading when a generator outage occurs at the PS-B power station (Region-B) it indicates a ROCOF of -0.29 Hz/s and a frequency nadir of 49.76 Hz for Region-B; these values are reduced to -0.30 Hz/s and 49.75 Hz when an outage occurs at the PS-A power station (Region-A). This is because during a PS-A generator outage the load centres are much closer to the outage, and hence the impact on generation-demand imbalance is considerably severe than a generator outage at a remote location. Furthermore, the aforementioned CCGT dynamic response also has a detrimental impact on the frequency stability of the system.

V. DISCUSSION

This study have shown that frequency stability detrimentally affected (large ROCOF and frequency nadir) when a fault occurs at the 275 kV network, in particular in close proximity to synchronous generation due to a large voltage impact across a wide area of the network (during frequency increase) and CCGT turbine response (during decrease). In addition, frequency stability is detrimentally threatened during grid faults due to combined wind power-CCGT interaction in the system. The resulting impact is two fold:

i. During initial frequency increase (at the fault instance) due to substantial voltage reduction at generator terminals (as illustrated in Fig. 7) generators accelerate while continuously increasing the system frequency. The terminal voltage reduction is mainly caused due to wind generation. This may be further exacerbated due to aforementioned CCGT dynamics during a frequency increase and ultimately may lead to a CCGT turbine combustor lean-blowout condition.

ii. Following fault clearance, system frequency substantially decreases with a large ROCOF and a frequency nadir due to wind generator slow recovery response (mainly DFIGs), wind generator tripping and comparatively large reduction in the CCGT power output.

These conditions are further exacerbated during high wind generator loading levels and base-load CCGT units.

VI. CONCLUSIONS

Frequency stability was analyzed during grid faults and generator outage events during high wind-CCGT penetrations in a test network. In particular, during grid faults significant CCGT-wind interaction has been observed (due to wind farm disconnection, slow recovery response of the DFIG wind generators and the CCGT response), which may lead to large frequency excursions during high wind and CCGT penetrations. This may be detrimental to system stability, since high ROCOF values have been observed and may give rise to potential CCGT 'lean-blowout', as occurred in the Florida power network in 2008. The base-load operated CCGTs further deteriorate the frequency stability of the network due to high active power output reduction (as a consequence of large fuel flow reduction to the combustor). However, frequency stability impact is much less during generator outage events in the network since FSIGs in the network provide adequate inertial response during a frequency decrease. Increasing penetration levels in renewable power generation in islanded systems such as New-Zealand and Ireland, these issues becoming increasingly important and hence future studies will analyze the sensitivity of wind penetration level on frequency dynamics for networks with high thermal generation.

VII. REFERENCES

[1] Global Wind Energy Council, *Global Wind Report 2010*, Apr. 2011. [Online]. Available: http://www.gwec.net.

[2] B. Fox, D. Flynn, L. Bryans, N. Jenkins, D. Milborrow, M. O' Malley, R. Watson, *Wind Power Integration: Connection and System Operational Aspects*. IEE Power and Energy Series 50, IET: London, 2007.

[3] G. Lalor, J. Ritchie, D. Flynn, M. J. O'Malley, "The impact of combined-cycle gas turbine short-term dynamics on frequency control," *IEEE Trans. Power Syst.,* vol. 20, no. 3, pp. 1456- 1464, Aug. 2005.

[4] Florida Reliability Coordinating Council, *FRCC System Disturbance and Under Frequency Load Shedding Event*, Nov. 2008. [Online]. Available: https://www.frcc.com.

[5] North American Electric Reliability Council, *Industry Advisory: Turbine Combustor Lean Blowout*, Jun. 2006. [Online]. Available: http://www.nerc.com.

[6] J. Morren, S. W. H. de Haan, W. L. Kling, J. A. Ferreira, "Wind turbines emulating inertia and supporting primary frequency control," *IEEE Trans. Power Syst.,* vol. 21, no. 1, pp. 433- 434, Feb. 2006.

[7] IEEE Task Force on Load Representation for Dynamic Performance, "Load representation for dynamic performance analysis," *IEEE Trans. Power Syst.*, vol. 8, no. 2, pp. 472-482, May 1993.

[8] W. W. Price, K. A. Wirgau, A. Murdoch, J. V. Mitsche, E. Vaahedi, M. A. El-Kady, "Load modelling for power flow and transient stability computer studies," *IEEE Trans. Power Syst.*, vol. 3, no. 1, pp. 180-187, Feb. 1988.

[9] The Irish Wind Energy Association, "NI transmission issues," *NIE Wind Workgroup*, Oct. 2008. [Online]. Available: http://www.soni.ltd.uk.

[10] L. Meegahapola, T. Littler, and D. Flynn, "Decoupled-DFIG fault ride-through strategy for enhanced stability performance during grid faults," *IEEE Trans. of Sust. Energy*, vol. 1, no. 3, pp. 152-162, Oct. 2010.